Low-Speed Aerodynamics of Apex Fences on a Tailless Delta Configuration

Keith D. Hoffler* and Dhanvada M. Rao†
Vigyan Research Associates Inc., Hampton, Virginia
and
Mark C. Frassinelli‡
AFWAL/FIMM, Wright-Patterson Air Force Base, Ohio

Apex fences are highly swept, upper-surface spoiler-like surfaces hinged at the leading edges of a delta wing. The fences are deployed vertically to generate a strong pair of counterrotating vortices at low angles of attack when the main-wing vortex system is weak. The intense suction induced by the fence vortices on the wing apex area creates a nose-up moment that, in conjunction with trailing-edge flaps, will enhance the trimmed-lift capability, thus reducing landing speed. Conversely, at high angles of attack, when the basic delta wing apex is highly loaded, the fences reduce the apex lift, resulting in pitch-down acceleration for a rapid return to normal flight attitude. These hypothesized characteristics of the apex fence concept were validated through low-speed tunnel experiments on a 60-deg delta wing configuration using flow visualization techniques, upper-surface pressure surveys, and balance measurements. This paper presents selected results of the investigation indicating the quantitative benefits that can be realized by the application of apex fences to tailless delta aircraft.

Nomenclature

A_R	=	fence-to-wing area ratio
Average *CPU*	=	span-averaged *CPU* at local chord station
C_{l_β}	=	β derivative of rolling moment coefficient (per degree)
C_L	=	lift coefficient based on total wing area
C_M	=	pitching moment based on total wing area and mean aerodynamic chord
C_{n_β}	=	β derivative of yawing moment coefficient (per degree)
CPU or $C_{P,U}$	=	upper-surface pressure coefficient
C_R	=	root chord, in.
L/D	=	lift-to-drag ratio
Re	=	Reynolds number based on mean aerodynamic chord
T	=	thrust, lb
V	=	approach velocity, knots
X	=	chordwise distance measured from apex, in.
Y-LOC	=	spanwise distance from root nondimensionalized by the local semispan
α	=	angle of attack, deg
β	=	sideslip angle, deg
γ	=	flight-path angle, deg
ΔC_L	=	(C_L, fence on $-C_L$, fence off)/(C_L, fence off)
δ_{fence}	=	fence deflection, deg

Subscript

T	=	value trimmed with trailing-edge flap

Introduction

THE tailless delta has been identified as a promising configuration for supersonic tactical aircraft, in view of its low wave drag, efficient structure, internal volume, and external load capacity, as exemplified in the F-16XL prototype. Against these advantages is the relatively limited aerodynamic control and trim power notably about the pitch axis, which so far has constrained the use of powerful trailing-edge high-lift devices needed to reduce the approach speed of tailless deltas. Lack of adequate pitch-down authority at high angles of attack, particularly in the context of relaxed or negative static stability, also limits the maneuver envelope. There is considerable interest, therefore, in exploring alternative pitch control systems for application to the tailless delta configuration, especially by using aerodynamic surfaces that may be conformally folded in high-speed flight so as not to compromise the inherent low-drag advantage of the basic configuration.

The apex region would appear to be a logical placement for a delta wing pitch surface, being farthest from the center of gravity and also where effective control on the natural delta wing vortices can be exercised at all angles of attack. Thus, modulation of vortex lift over the apex region (defined as all of the wing area forward of the center of gravity) can furnish both positive and negative pitching moment increments. The apex flap investigated in Ref. 1 represented one embodiment of this approach. This paper deals with another apex-lift modulation concept – the apex fence.

Resembling highly swept spoilers, the apex fences are hinged to the wing upper surface along the leading edges (Fig. 1). When unfolded vertically at low angles of attack, the fences generate a strong counterrotating pair of vortices whose suction augments lift in the apex region, resulting in a nose-up moment. Conversely, at high angles of attack, the fence vortices become weaker and also are raised well above the apex; the combined effect then is to reduce the apex lift, thus generating a desirable nose-down moment. The apex fences will not be subject to fuselage interference and they may be shaped and the hinge position oriented for most efficient vortex generation independently of the wing planform.

Exploratory small-scale wind-tunnel investigations of the apex fence concept applied to a 74- and 65-deg delta wing were reported in Ref. 2. Upper-surface pressure surveys supplemented with oil-flow and helium-bubble visualizations confirmed the existence of strong and stable vortices produced by apex fences. These promising early results encouraged a more comprehensive study of the concept applied to a 60-deg delta wing; this wing sweep angle being more in tune with the cur-

Presented as Paper 86-1838 at the AIAA 4th Applied Aerodynamics Conference, San Diego, CA, June 9–11, 1986; received July 21, 1986; revision submitted March 11, 1987.

*Research Engineer. Member AIAA.
†Vice President. Associate Fellow AIAA.
‡Airplane Aerodynamics Engineer, Flight Dynamics Laboratory.

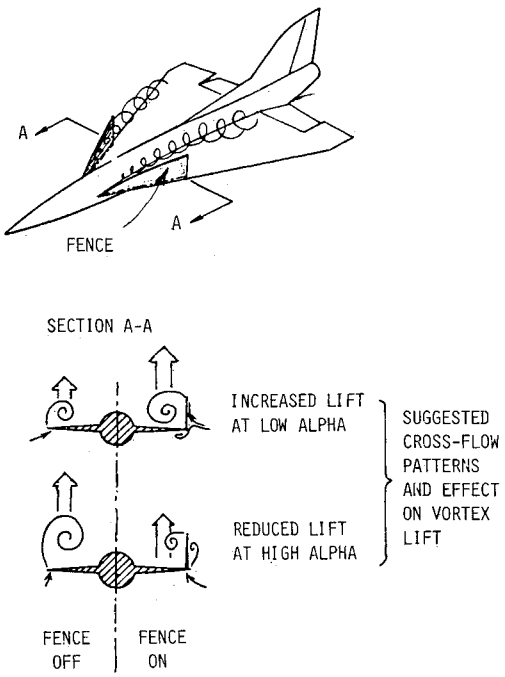

Fig. 1 Apex fence concept.

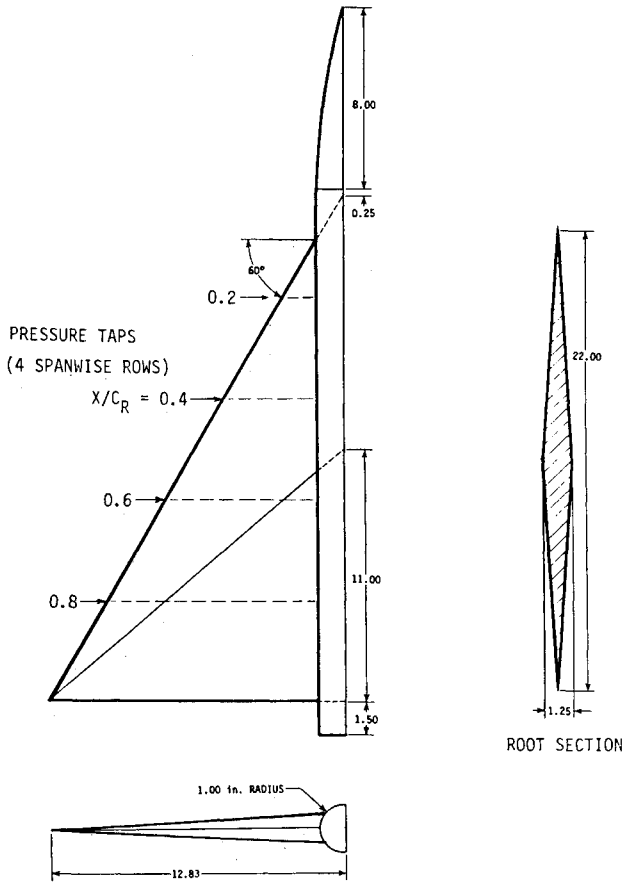

Fig. 2 Sixty-degree Delta wing semispan pressure model tested at North Carolina State University.

rent fighter design studies. The present investigation was undertaken to validate the concept and quantitatively evaluate the aerodynamic potential of apex fences for improving primarily longitudinal, and possibly lateral/directional, characteristics of a tailless delta through the angle-of-attack range.

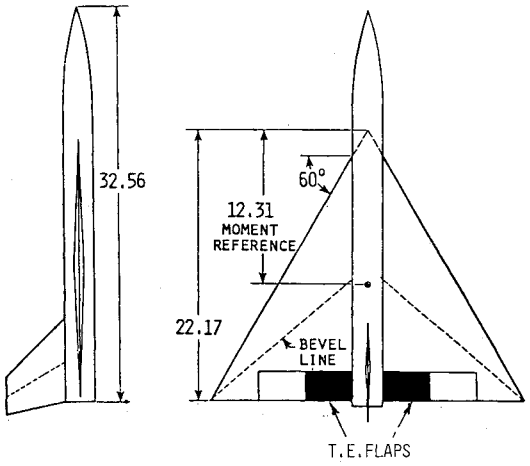

Fig. 3 Sixty-degree Delta wing force model tested in AFIT 5-ft wind tunnel.

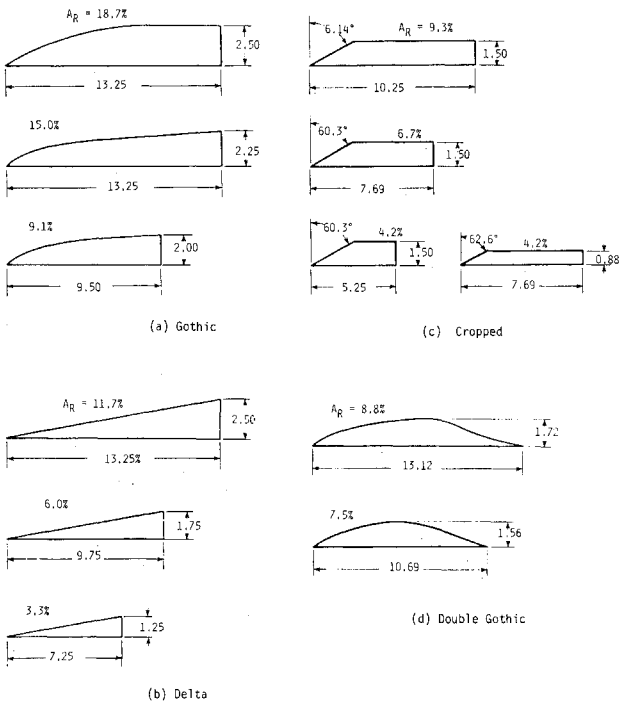

Fig. 4 Fence shapes investigated showing fence area and major dimensions.

Wind-Tunnel Models and Test Details

Pressure Model

Major dimensions of the semispan 60-deg delta wing body model are shown in Fig. 2. This model incorporates four spanwise rows of pressure taps on the upper surface, the first row being well inside the apex region occupied by the fence. The model was mounted on a boundary-layer bypass plate 7 in. above the tunnel floor. Six fence shapes were tested on this model. The test was conducted in the North Carolina State University Merrill Subsonic Wind Tunnel at a mean aerodynamic chord (mac) Reynolds number of 0.67×10^6 and angles of attack ranging from 0 to 30 deg. Helium-bubble/flow-visualization studies were conducted on this model at a mach Reynolds number of 0.11×10^6.

Force Model

Major dimensions of the force model are shown in Fig. 3. This model was geometrically similar to the pressure model and was fitted with four trailing-edge flaps. Only the inboard

flap segments were deflected during the present tests. A total of 12 fence shapes were investigated, some at different mounting positions on the wing and some in asymmetric arrangement. The test was conducted in the Air Force Institute of Technology 5-ft Subsonic Wind Tunnel at a mean aerodynamic chord Reynolds number of 1.11×10^6. The sting was mounted in two alternate positions, giving a low (-6–30 deg) and a high (20-48 deg) angle-of-attack range. Oil-flow studies were also conducted on this model.

Fences

The major dimensions of the 12 fences tested are shown in Fig. 4. Not all the fence shapes on the force model were included in the pressure study. The fences were mounted with the hinge line along the leading edge and, unless otherwise noted, deflected at 90 deg (i.e., perpendicular to the wing plane).

Results and Discussion

Helium-Bubble/Flow-Visualization Study

A typical helium-bubble photograph showing the leading-edge-mounted Gothic fence at 75-deg deflection and 10-deg angle of attack is presented in Fig. 5. The presence of a strong vortex formed by the Gothic fence is evidenced by the tightly wound (dark) core in the fence region. This vortex would be expected to induce a high suction in the apex region. Downstream persistence of the fence vortex suggests that wing lift would be maintained to some degree. The visualizations qualitatively supported the fence vortex flow postulated in Fig. 1.

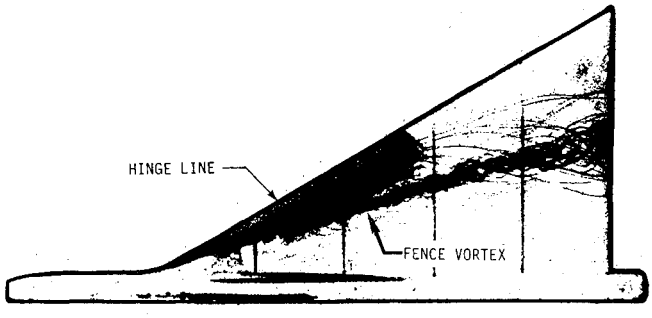

Fig. 5 Helium-bubble flow visualization showing fence vortex.

Pressure Results

Typical spanwise pressure distributions resulting from vertical apex fences at the leading edge of the delta wing will be examined at a constant α of 10 deg (representing a low-α case). The Gothic (18.7% area) fence (Fig. 6) produces a broader suction footprint at the first two pressure stations (A and B) and a significant increase of the span-averaged local $-C_{P,U}$ relative to the basic wing, while the load center is shifted inboard. At the downstream stations (C and D), the spanwise distribution is similarly altered but the average $-C_{P,U}$ is somewhat reduced. Note the evidence of a leading-edge vortex distinct from the fence vortex at the last chord station. The effects with the Delta (11.7% area) fence (Fig. 7) are basically similar, with noteworthy differences being that the suction peaks are more accentuated in this case while the vortex footprints are not as broad as with the Gothic fence. Nevertheless, the resulting span-averaged $-C_{P,U}$ values are practically identical in the two fence configurations. At the downstream stations, the difference between the respective pressure fields is insignificant.

The longitudinal variation of $-C_{P,U}$ (average) presented in Fig. 8 clearly shows the fence-augmented suction in the apex region at α = 10 deg. Just the opposite occurs, however, at α = 30 deg (representing a high-α case); the apex suction being reduced below the basic wing value. Accordingly, a nose-up moment increment at low α and a nose-down increment at high α are to be expected due to fence deployment, as postulated. This trend of reversing pitching moment, as encountered in varying degree with all the fence configurations tested, is unique to the apex fence concept.

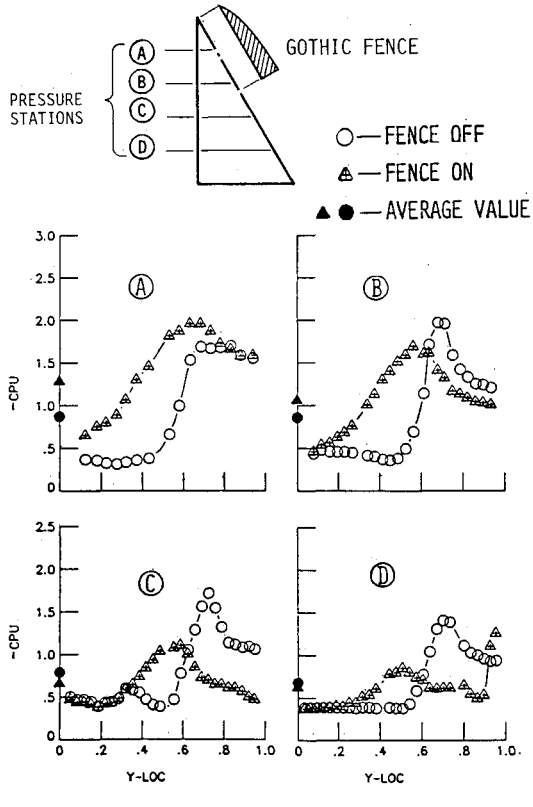

Fig. 6 Spanwise distribution of upper-surface pressures with largest Gothic fence (α = 10 deg.)

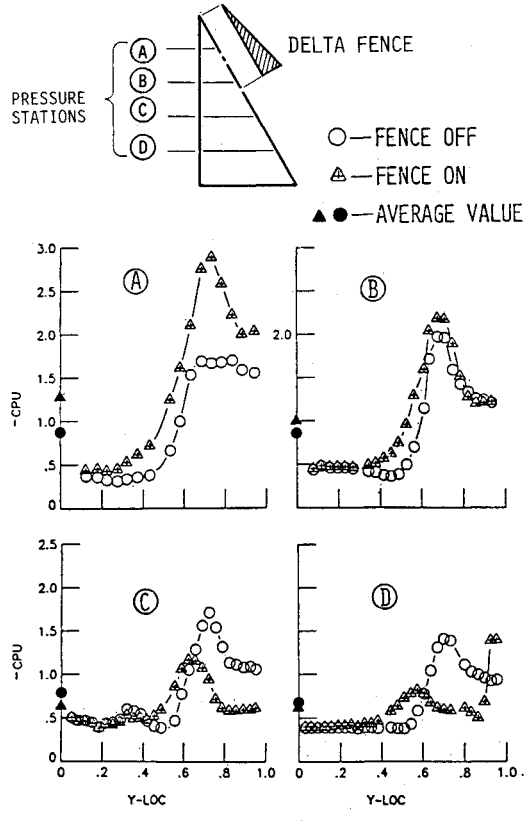

Fig. 7 Spanwise distribution of upper-surface pressures with largest Delta fence (α = 10 deg).

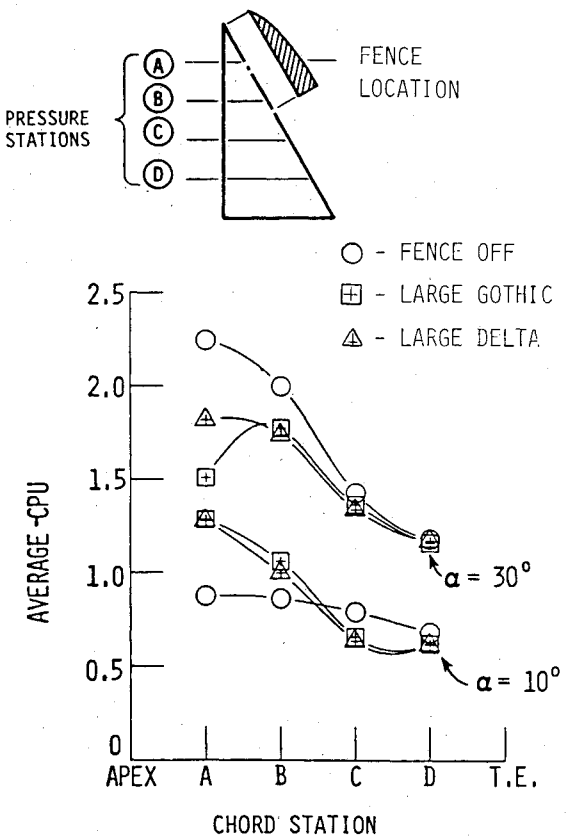

Fig. 8 Longitudinal distributions of span-averaged upper-surface pressure coefficients.

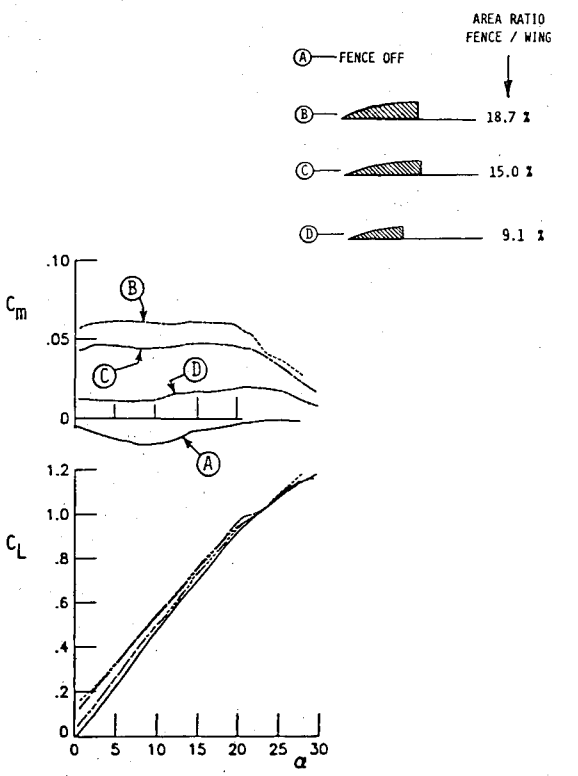

Fig. 9 Effect of Gothic fence area variation on lift and pitching moment.

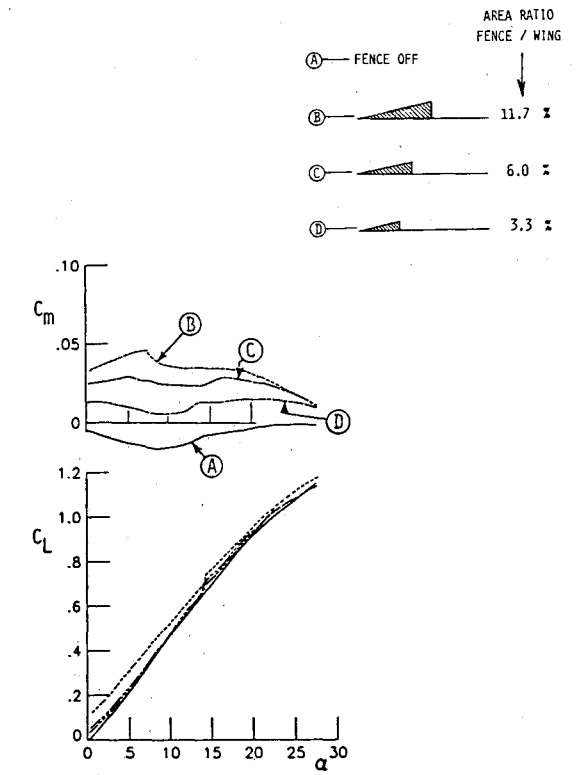

Fig. 10 Effect of Delta fence area variation on lift and pitching moment.

Balance Results

Fences belonging to two shape families, viz., Gothic and Delta, and varying in area were investigated initially. The fence deflection in these tests was 90 deg (i.e., perpendicular to the wing plane). The lift and pitching moment results for the two shape families are shown in Figs. 9 and 10. The lift increment due to the fences is essentially concentrated in the apex region (as seen in the previous study) since it generates a positive pitching moment. The pitching moment increment is practically constant up to 20-deg angle of attack and, generally, its magnitude is proportional to the fence area. No clear-cut effects of the fence shape could be discerned in this limited data set.

The fence-generated nose-up pitching moment increments were balanced with the nose-down moment measured with a deflected trailing-edge flap on the basic model to obtain the trimmed-lift characteristics. A comparison of the trimmed-lift coefficient for the various fence configurations at $\alpha = 12$ deg is presented in Fig. 11. The lift increment is primarily due to trailing-edge flap contribution; the different fences requiring different levels of trimming moment. The lift improvements generally are found to be in proportion to the fence area. The fence-on trimmed-lift increment is plotted versus the percent fence-to-wing area in Fig. 12 in an attempt to identify a particularly efficient fence shape. Based on a single data point, the Double Gothic shape seems to point the way toward improving the fence area efficiency. The present data base, although inconclusive, does suggest that further studies dedicated to fence shape refinement should be worthwhile.

Trimmed-lift coefficients of three of the fences through the low-α range are shown in Fig. 13a. The trimmed-lift increment is maintained with all three fences to $\alpha = 20$ deg before gradually tapering off. Because the positive static margin of the basic delta wing requires an up-deflected trailing-edge flap to trim, the angle of attack must be increased for the same lift coefficient. In contrast, fence deployment allows a down is desirable during approach and landing, it is still of interest trailing-edge flap deflection for trim and, therefore, the angle of attack can be reduced for the same approach speed. For example, the Gothic fence provides nearly a 6-deg reduction of the angle of attack from the basic wing at a trimmed-lift coefficient of 0.5.

The vortex load on the apex fences produces a drag component. While a drag increment in conjunction with increased lift

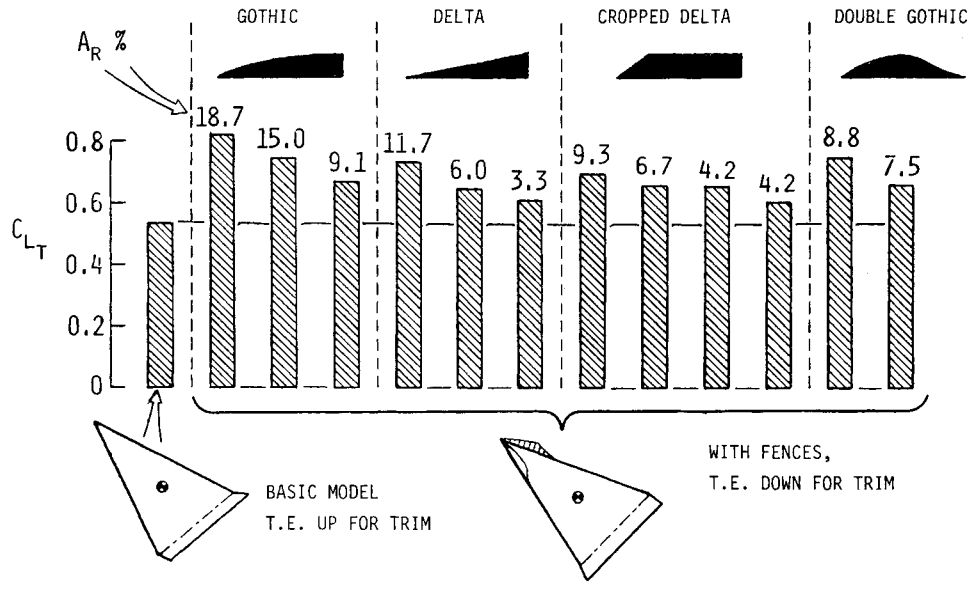

Fig. 11 Trimmed-lift coefficient at α = 12 deg with various fence shapes and area.

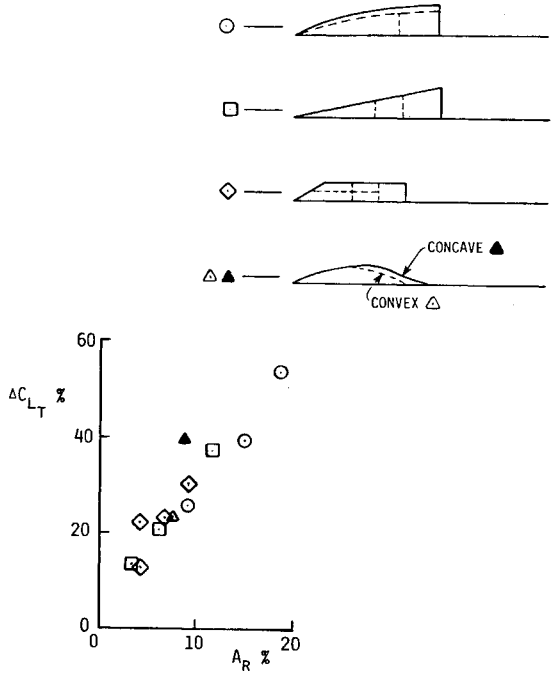

Fig. 12 Trimmed-lift increment at α = 12 deg as a function of fence-to-wing area ratio.

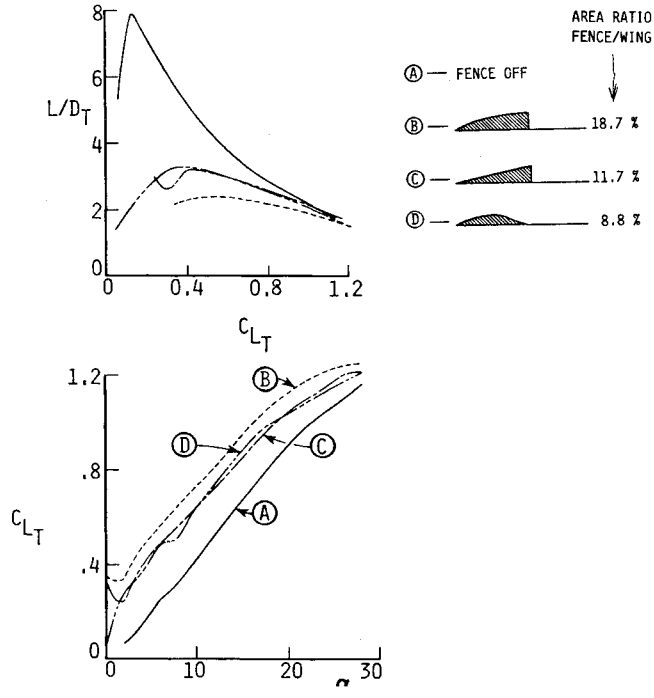

Fig. 13 Comparison of trimmed-lift and trimmed L/D characteristics for three fence shapes.

to examine the aerodynamic efficiency of apex fences as a trimming device. This may be done by plotting L/D_T vs C_{L_T} with and without fences (see Fig. 13b). At high-lift coefficients, L/D_T with and without the fences are nearly equal. This is due to a lower α required to obtain the same lift coefficent as already noted; the reduced wing drag then compensates for the fence drag to a large extent.

The hinged fences may be deployed to a smaller or larger angle than the 90 deg used in the preceding tests. The effect of varying fence deflection on either side of 90 deg is presented in Fig. 14 for the Double Gothic fence. The results indicate that the fence angle controls the pitching moment in an almost linear fashion.

The high-α range was explored to observe the apex fence effect on pitching moment. Typical results are shown in Fig. 15 using the Large Gothic, Large Delta, and Double Gothic fences, where a sign change in the pitching moment increment is evident at high angles of attack. The alpha for this change ranged from approximately 28 to 40 deg, depending on fence size and shape. Thus, apex fences can be viewed as a natural α-limiting device.

In sideslip, the apex fences may be expected to produce pronounced effects on the lateral/directional characteristics of the basic wing. Lateral/direction derivatives with the largest Gothic fence and planar wing are shown in Fig. 16. As suggested in the sketch, the sideforce on the windward fence decreases because its vortex moves away from the fence, while the opposite occurs on the leeward fence; the net sideforce thus generating a stabilizing yawing moment. At the same time, a stabilizing rolling moment is generated presumably due to a strong leading-edge vortex developing on the windward side of the wing. These favorable effects obtained at β = 3 deg are expected to change at large sideslip angles, i.e., β approaching the wing semiapex angle.

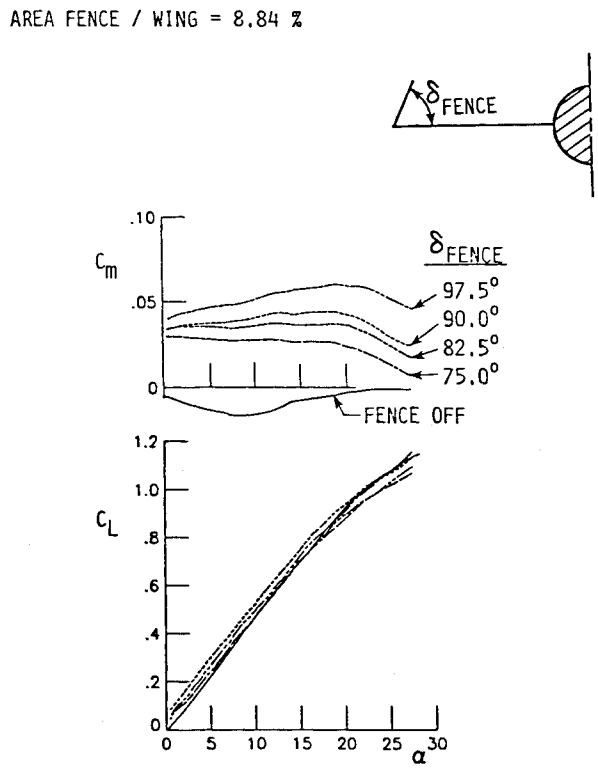

Fig. 14 Effects of fence deflection angle on lift and pitching moment.

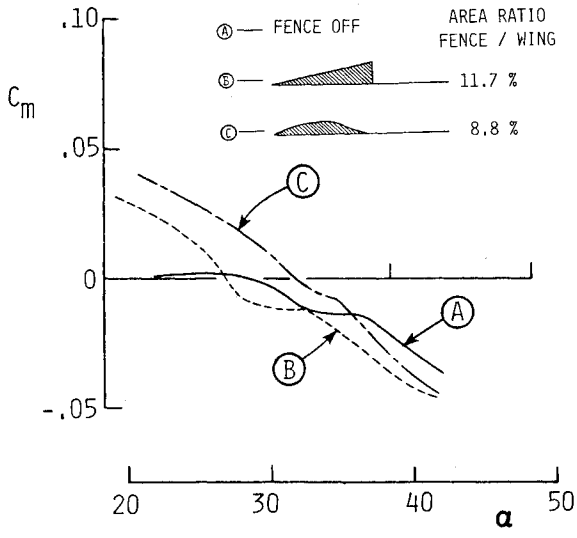

Fig. 15 Fence effect on pitching moment at high angles of attack.

Since the apex fence offers large benefits to a tailless delta configuration, some rough calculations of the approach speed reduction of an actual aircraft would be of interest. A Convair F-106A was chosen because its pure 60-deg delta planform is similar to the model used in the current investigation. The results of these calculations are shown in Fig. 17 for the Large Gothic, Delta, and Double Gothic fences. The Large Gothic fence produced the greatest reduction in approach speed but also the greatest increase in thrust. The thrust increase required by this fence is unacceptable because it is almost in the afterburner range of the F-106's engine. The other two fences produced a 20% reduction in approach speed (36 kn) with more reasonable increased thrust requirements. Note that a high-power setting is desirable on approach in case an aborted landing is necessary and for deceleration if thrust reversing is available. Therefore, the use of apex fences on approach can

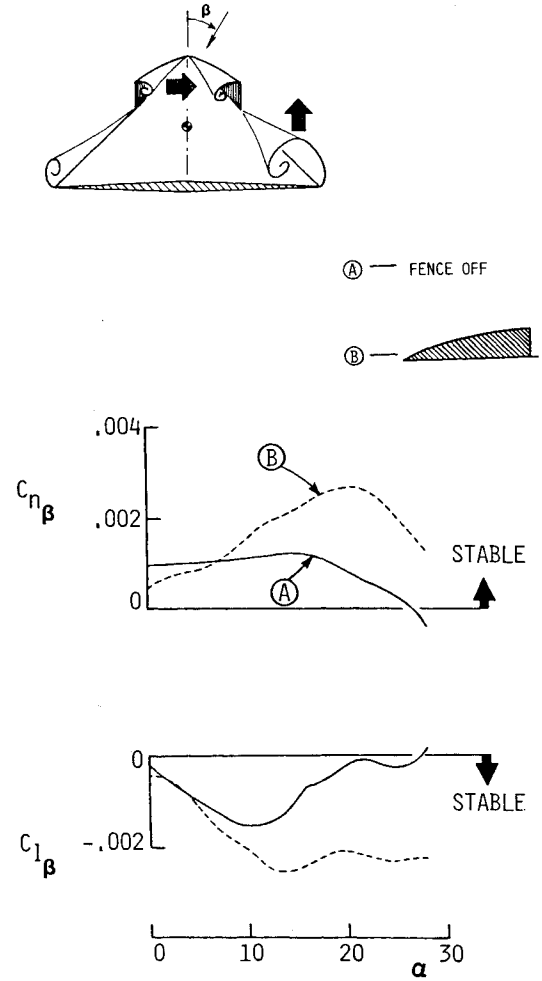

Fig. 16 Lateral and directional stability derivatives showing effect of Gothic fence.

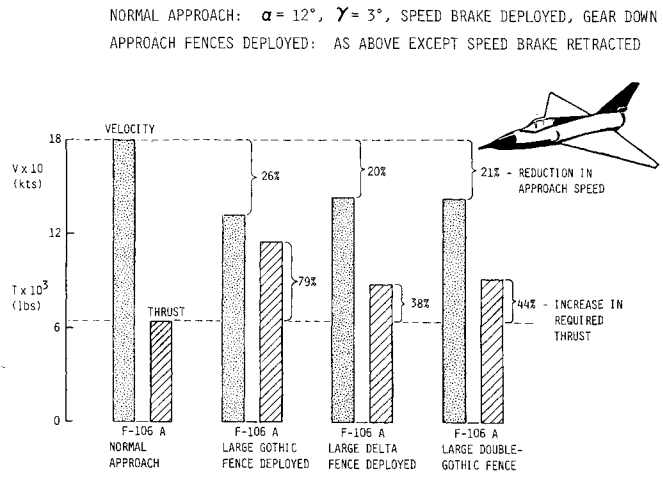

Fig. 17 Estimated effect of three fences on landing approach speed and thrust level of F-106A.

reduce approach speed, further reduce ground roll, and improve safety via increased power setting and improving lateral/directional stability.

Conclusions

Exploratory low-speed wind-tunnel investigations were conducted to evaluate the effects of apex fences on a 60-deg delta wing/body configuration. An initial test program surveyed upper-surface pressures on a semispan model, including the

apex region between the fences, followed by balance measurements on a geometrically similar full-span model with trailing-edge flaps. The scope of the investigation covered varying fence shape, area, and deflection angles.

The apex fences produced opposite lift effects over the wing-apex region in the low-α and high-α regimes, as postulated. At angles of attack less than approximately 25 deg, fence vortices augmented the suction level over the apex, whereas at higher angles of attack the apex suction was reduced below the basic wing case. Balance data showed a corresponding lift increase due to fences together with a nose-up pitching moment at low α and a lift loss together with nose-down moment at high α.

In combination with down-deflected trailing-edge flaps, the fences produced marked increases in the trimmed-lift capability of the configuration particularly in the low-α range. The increment in trimmed lift was generally proportional to the fence/wing area ratio; however, one fence shape, viz., the Double Gothic, appeared to be more area efficient than the others.

Varying fence deflection angle (on either side of the nominal 90-deg position) was found to control the pitching moment in a linear fashion, showing the apex fence to be a promising pitch control and trimming device. The fences improved lateral/directional stability, at least at small sideslip angles.

Calculations showed the fences to be capable of reducing the approach speed of an F-106A by 20% without increasing the angle of attack. Other benefits that would be realized on approach are increased power setting, improved lateral/directional stability, and decreased ground roll.

Acknowledgments

This research was supported by the Air Force Flight Dynamics Laboratory, Wright-Patterson Air Force Base, under Contract FY-1456-85-00032. Considerable assistance in conducting the wind-tunnel test was received from Lt. M. Stuart and Capt. C. Smith, graduate students of the Air Force Institute of Technology (AFIT), which is greatly appreciated. The authors extend their gratitude to AFIT for the use of a model, the 5-foot tunnel facility, and associated personnel. The assistance of Mr. T. Mills, Vigyan Research Associates Inc., in data reduction and the North Carolina State University wind-tunnel test is greatly appreciated.

References

[1]Rao, D.M. and Buter, T.A., "Experimental and Computational Studies of a Delta Wing Apex Flap," AIAA Paper 83-1815, July 1983.

[2]Wahls, R.A. and Vess, R.J., "An Exploratory Study of Apex Fence Flaps on a 74 deg Delta Wing," NASA CR 172463, May 1985.